申请专业学位研究生校内指导教师佐证材料

申请人姓名：高立学

专业学位类别：临床医学

专业学位领域：外科学

工 作 单 位 ：保定市第二医院

2025 年 5 月

目 录

（“目录”黑体、二号；一级标题，如“学历、资历”，黑体、小四号；其它内容，宋体，五号。整篇 1.25 倍行距。）

姓名 高立学

性别 男 民族 汉

出生 1969 年 8 月 3 日

住址

公民身份号码

中华人民共和国

居民身份证

签发机关 保定市公安局北市分局

有效期限 2008.03.20-2028.03.20

①

文凭登记第931271号

毕业文凭

学生高立学，男，现年23岁，

系河北省(市)雄县人，于一九

八八年九月至一九九三年七月

在本院临床医学系本科学习五年，修业

期满，成绩及格，准予毕业。

院长 [illegible]

一九九三年七月十日

硕士学位证书

高立学，男，1969 年 8 月 3 日生。在 华北煤炭医学院 外科学 学科（专业）已通过硕士学位的课程考试和论文答辩，成绩合格。根据《中华人民共和国学位条例》的规定，授予 医学 硕士学位。

华北煤炭医学院

院　长
学位评定委员会主席 袁聚祥

证书编号：T1009032009000255

二OO九 年 六 月 三十 日

专业技术系列 卫生
Professional Series

专业名称 医疗
Name of Speciality

资格名称 主任医师
Name Qualification

批文号 冀职改办字【2011】224号
Approval No.

授予时间 2011.12.22
Date of Conferment

工作单位 保定市第二医院
Work Unit

BDKW1110810

③

(加 效)

姓名 高立学 性别 男
Name Sex

出生年月 1969.08.03
Date of Birth

编号 0299383
No.

二〇一二年 三月 七日

奖励证书

保定20164186-3号

为表彰在科技工作中取得优异成绩者，特发此证，以资鼓励。

受奖者 高立学（第叁完成人）

受奖项目 乌司他丁联合参麦注射液治疗急性胰腺炎疗效观察

受奖级别 科技进步二等奖

保定市科学技术和知识产权局

2016年6月8日

Biochemical Genetics
https://doi.org/10.1007/s10528-021-10180-6

ORIGINAL ARTICLE

Exosomal circ_0001190 Regulates the Progression of Gastric Cancer via miR-586/SOSTDC1 Axis

Chao Liu[1] · Jing Yang[2] · Fengchi Zhu[2] · Zhiying Zhao[1] · Lixue Gao[3]

Received: 2 September 2021 / Accepted: 20 December 2021

Abstract

Gastric cancer (GC) is the fifth most common cancer, which has a significant impact on human health. Recent researches have shown that circular RNAs (circRNAs) could affect the progress of GC, but the mechanism still indistinct. In this work, we explored the roles of circ_0001190 in GC. The levels of circ_0001190, microRNA-586 (miR-586) and sclerostin domain containing 1 (SOSTDC1) were detected by quantitative RT-PCR and western blot in GC. The cell functions were scrutinized by cell counting kit-8 assay, 5-Ethynyl-29-deoxyuridine assay, flow cytometry assay, tube formation assay, transwell assay, and western blot. Furthermore, the relationship between miR-586 and circ_0001190 or SOSTDC1 was identified by dual-luciferase reporter assay. Finally, the xenograft model test was implemented to demonstrate the effect of exosomal circ_0001190 in vivo. The levels of circ_0001190 and SOSTDC1 were downregulated, and the miR-586 level was increased in GC. For functional assay, circ _0001190 overexpression inhibited cell vitality, cell proliferation, angiogenesis, cell migration and invasion, whereas stimulated cell apoptosis in GC cells. Circ _0001190 served as a miR-586 sponge to adjust the expression of SOSTDC1. Additionally, miR-586 could promote the advancement of GC by interfering SOSTDC1. Exosomal circ_0001190 overexpression inhibited the development of GC by miR-586/SOSTDC1 axis, which proposed a potential targeted therapy for GC cure.

Keywords Gastric cancer · Exosomal circ_0001190 · miR-586 · SOSTDC1

✉ Lixue Gao
wkysglx@163.com

[1] Department of Gastroenterology, the No 2 Hospital of Baoding, Baoding City 071051, Hebei, China

[2] Department of Anorectal Surgery, the No 2 Hospital of Baoding, Baoding City 071051, Hebei, China

[3] Department of Surgical Oncology, the No 2 Hospital of Baoding, No.338 Dongfeng West Road, Baoding City 071051, Hebei, China

Published online: 09 February 2022

5

Introduction

Gastric cancer (GC) is a common cancer and its mortality is the second worldwide (Bray et al. 2018; Song et al. 2017). The five-year survival rate of GC is 20%–40% (Allemani et al. 2018). Analysis of the age of onset in recent years showed that the risk was increased in younger people (Lee et al. 2017). Patients with GC have the characteristics of high metastasis rate and mortality, and the effect of current treatment methods is not ideal (Sun et al. 2015). Therefore, we urgently need to find a new way for GC treatment.

Circular RNAs (circRNAs) are a kind of RNAs that have no 5'-caps and 3'-tails, which can stably exist in plentiful types of organisms and play important roles in various cellular processes (Ambros 2004; Garzon et al. 2010). For instance, hsa_circ_0004872 overexpression hindered the invasion and migration of GC cells (Ma et al. 2020). Besides, hsa_circ_006100 stimulated cell growth and metastasis (Liang 2019). In addition, circ_0000190 induced apoptosis and cell cycle arrest in GC (Wang et al. 2020a). Previous studies have shown that circ_0001190 was significantly downregulated in both tumor tissues and plasma of GC patients (Liu et al. 2020; Li et al. 2018). Therefore, we speculated that circ_0001190 was of great significance to the growth of GC. However, the functions of circ_0001190 on GC is ill-defined.

MicroRNAs (miRNAs) are a type of small RNAs, which regulates the subsequent biology processes (Ambros 2004; Garzon et al. 2010). For example, miRNA-586 low expression was a mark of poor prognosis in glioma (Luo et al. 2020). Moreover, miR-21 took part in regulating cisplatin resistance in GC (Zheng et al. 2017). In addition, miR-129-5p inhibited cell proliferation in GC (Wang and Yu 2018). However, the understanding of the influence of miR-586 in GC still restricted.

Previous studies have shown that sclerostin domain containing 1 (SOSTDC1) played an indispensable role in the formation of teeth, hair follicles, and trigeminal ganglion (Ahn et al. 2017; Narhi et al. 2012; Shigetani et al. 2008). In addition, SOSTDC1 was involved in regulating cell differentiation and proliferation (Chen et al. 2018). Moreover, SOSTDC1 inhibited cell migration in follicular thyroid cancer (Zhou et al. 2017). However, the relationship between SOSTDC1 and the GC is still indistinct, which is worth studying in detail.

In this paper, we studied the molecular regulation mechanism of circ_0001190 in GC. The research revealed that circ_0001190 suppressed the progression of GC. Our consequences might provide innovative ideas for targeted therapy of GC and provide molecular theoretical basis for subsequent clinical treatment.

(6)

Materials and Methods

Clinical Tissue Samples

The research was approved by the No 2 Hospital of Baoding. Forty pairs of GC tissues were employed to qRT-PCR. In addition, blood samples from 10 GC sufferers and 10 healthy controls (not diagnosed with cancer) were collected for exosome extraction. All samples were gathered from the No 2 Hospital of Baoding. All the volunteers signed informed consent forms. Afterward, all samples were conserved at − 80 °C.

Cell lines and Cell Culture

The human GC cell lines (HGC27, AGS, MKN45, MKN47 and N87), with GES-1 cells as control. Human Umbilical Vein Endothelial Cells (HUVECs) were used for tube formation assay. All cells were bought from Cell Bank, Chinese Academy of Sciences (CAS, Shanghai, China). These cells were cultivated with RPMI 1640 medium (Gibco, Carlsbad, CA, USA) and F12K medium (Gibco, only for AGS) in 5% CO_2.

Exosome Isolation and Identification

Exosomes from cells are collected from cell culture medium or serum. As described by Xie et al., the cell culture medium or serum was centrifuged and the product was washed (Xie et al. 2020). Then ExoQuick Exosome (SBI, CA, USA) precipitated solution was added according to the instructions, refrigerated and centrifuged, and sterile PBS was used to re-suspend exosome particles. Finally, transmission electron microscopy was used to identify the size and form of exosomes. The particle size was detected by Nanoparticle tracking analysis (NTA). Exosome protein markers were assessed by western blot analysis.

Quantitative RT-PCR

RNA was separated by Trizol (Sigma-Aldrich, St. Louis, MO, USA). Whereafter, entire RNA was reverse-transcribed to complementary DNA. The Prime Script RT reagent kit (Thermo Fisher Scientific, Waltham, MA, USA) was applied for circ_0001190 and SOSTDC1 reverse transcription. Meanwhile, miRNA was reverse-transcribed using a miRNA First-Strand Synthesis kit (Takara, Tokyo, Japan) for miR-586. Next, cDNA was applied for qRT-PCR with an SYBR Green kit (Takara). GAPDH and RNU6 (U6) were used as endogenous controls to standardize circRNA and miRNA expression levels, respectively. The primers are listed in Table 1. Relative abundance was computed by the $2^{-\Delta\Delta Ct}$ method.

Table 1 Primers sequences used for PCR

Name	Primers (5′-3′)	
circ_0001190	Forward	TGCAGGAACTATTTCTCAGCATTG
	Reverse	AAGAGTCCAGCGGCAAAACT
SOSTDC1	Forward	CCGTACCCAGAGAATCCAGC
	Reverse	ATTTGCTGGCTCTTTTCCGC
miR-586	Forward	GCCGAGTATGCATTGTATTTTTA
	Reverse	CTCAACTGGTGTCGTGGA
GAPDH	Forward	TCCCATCACCATCTTCCAGG
	Reverse	GATGACCCTTTTGGCTCCC
U6	Forward	CTCGCTTCGGCAGCACATATACT
	Reverse	ACGCTTCACGAATTTGCGTGTC
miR-576-5p	Forward	GCCGAGATTCTAATTTCTCCACG
	Reverse	CTCAACTGGTGTCGTGGA
miR-512-5p	Forward	CGGGCGGCACTCAGCCTTGAGGG
	Reverse	CTCAACTGGTGTCGTGGA
miR-1827	Forward	GGGGTGAGGCAGTAGATTG
	Reverse	CTCAACTGGTGTCGTGGA
miR-568	Forward	GCCGAGATGTATAAATGTATACACA
	Reverse	CTCAACTGGTGTCGTGGA
miR-665	Forward	GGTGAACCAGGAGGCTGAGG
	Reverse	CTCAACTGGTGTCGTGGA
DYRK1A	Forward	GTTCGGGCTCTCCTGGC
	Reverse	CTCAGTCTCTCCTCGGCTCG

Western Blot

The method of western blot was as previously reported (Hou and Zhang 2021). The GC cells were treated with a RIPA buffer (Sigma), and the protein content was assessed through a BCA kit (Sigma). The disconnected protein was moved to a 10% SDS-PAGE and therewith transferred to PVDF membranes (Sigma). Subsequently, the membranes were hatched with the nether primary antibodies: anti-CD9 (ab92726; 1:1000; Abcam, Cambridge, MA, USA), anti-CD63 (ab119992; 1:1000; Abcam), anti-TSG101 (ab125011; 1:1000; Abcam), anti-Ki67 (ab92742; 1:1,000; Abcam), anti-Bax (ab32503; 1:1,000; Abcam), anti-MMP-2 (ab92536; 1:1000; Abcam), anti-SOSTDC1 (SAB2107833; 1:1000; Sigma), and anti-β-actin (ab8226; 1:1000; Abcam). Conclusively, the membranes were hatched with a secondary antibody (ab205718; 1:2500; Abcam) for 1 h. Finally, the protein band was observed.

RNase R Degradation Assay

On the basis of the RNase R kit directions (Sigma), the RNA was treated with RNase R. Moreover, the DYRK1A mRNA was employed as control. The RNA

(5 μL) was disposed of RNase R (10 U, Sigma) for 30 min. At that moment, the levels of circ_0001190 and DYRK1A mRNA were detected.

Cell Transfection

The circ_0001190 exo, the control (vector exo), miR-586 mimic, and miR-NC, the si-SOSTDC1 and control (si-NC) were acquired from Ribobio (Guangzhou, China). These plasmids or oligonucleotides were transferred in into GC cells by utilizing Lipofectamine 2000 (Thermo Fisher Scientific).

CCK8 Assay

After post-transfection, GC cells (2.0×10^3/well) were planted in 96-well plates. Then, the CCK8 (20 μL, Sigma) was supplemented and nurture 4 h. The OD value was assessed at 450 nm to confirm the cell viability.

Cell Proliferation Assay

After transfection, GC cells were seeded into 96-well plates. Then, the EdU Apollo in Vitro Imaging Kit (RiboBio) was used as stated by the guide. GC cells were incubated with EdU and exposed to paraformaldehyde (4%; RiboBio) for 30 min. Following, the Triton X-100 and Apollo solution were added. In the end, cells were exposed to DAPI (RiboBio).

Flow Cytometry Assay

GC cells after varied transfection were planted in 96-well plates. As the described by Wang et al., the Annexin V-FITC Apoptosis Detection Kit (Sigma) was used to treat every group cells (Wang et al. 2020b). The apoptotic cells were observed under a flow cytometry.

Tube Formation Assay

HUVECs (4×10^5 cells/well) with different treatment were planted into Matrigel-coated 96-well plates. Meanwhile, the tube formation rate was examined after 24 h. Afterward, Image J software (NIH, Bethesda, MD, USA) was used to observe the number of tubes and the count of branches. The elongated multi-cellular structures were considered tube-like structures. The intersecting points of two or more tubes were considered branches.

Transwell Assay

After 48 h transfection, GC cells were performed in a transwell with 8 μm pore polycarbonate membrane (Corning, MA, USA). GC cells (4×10^5) were planted on the

9

upper chambers coated in serum-free medium. Then, 500 μL of DMEM comprising 10% FBS was added to the inferior chamber of the transwell. The same method was used, but transwell chamber precoated Matrigel (Corning) was implemented to evaluate the invasion. After 12 h, cells were fixed and exposed to crystal violet solution, and observed under a light microscope.

Dual-luciferase Reporter Assay

The binding site between miR-586 with circ_0001190 or SOSTDC1 was estimated by circinteractome (https://circinteractome.nia.nih.gov), circbank (http://www.circbank.cn/) and targetscan (http://www.targetscan.org). Then, the wild type and mutant circ_0001190 and SOSTDC1 were manufactured by Ribobio (circ_0001190 WT, SOSTDC1 3'UTR WT or circ_0001190 MUT, SOSTDC1 3'UTR MUT). The luciferase activity was tested.

RNA Pull-Down

The Bio-miR-586, Bio-miR-586 MUT, and control (Bio-NC) were manufactured by RiboBio. A RNA–Protein Pull-Down Kit (Sigma) was utilized to recognize the interaction among circ_0001190 and miR-586. After post-transfection, GC cells were nurtured with the probe-bead compound for 3 h. Next, the beads were collected, and removed the protein and DNA, respectively. Lastly, the level of circ_0001190 was measured.

Xenograft Models

The research was approved by the Animal Care and Use Committee of the No 2 Hospital of Baoding. All nude mice were got from Beijing Vital River Laboratory Animal Technology (Beijing, China). HGC27 cells (1×10^6) with circ_0001190 or the vector exo were inoculated into mice (female, two groups, n = 6/group, 6 weeks, 18–22 g). Lastly, tumor volume was registered once a week suitable for the formula: Tumor volume = length × width^2 × 0.5. After 35 days, the tumor tissues were carved for supplementary experiment.

Immunohistochemistry (IHC) Assay

The IHC was carried out as Qiu et al. described (Qiu et al. 2018). The slice was sealed by peroxidase and exposed to PBS that comprised 10% skim milk about 20 min to seal particular sites. The SOSTDC1 primary antibody (ab99340; 1:1,000; Abcam) and Ki67 (ab16667; 1:1,000; Abcam) were hatched. Next, the secondary antibody (ab150113, Abcam) conjugated with HRP was incubated for 30 min. Eventually, the slides were stained using diaminobenzidine (Sigma) and observed.

Statistical Assay

All data were obtained from no less than three independent reiterations and analyzed by SPSS 23.0 (SPSS, USA). Shapiro–Wilk test was used to check the normal distribution of all data. Pearson's correlation assay was implemented to reveal the correlation between two groups. Student's *t*-test was employed to examine the statistical differences between two groups, and ANOVA was administrated to compare the statistical differences among multiple groups. $P < 0.05$ was significant.

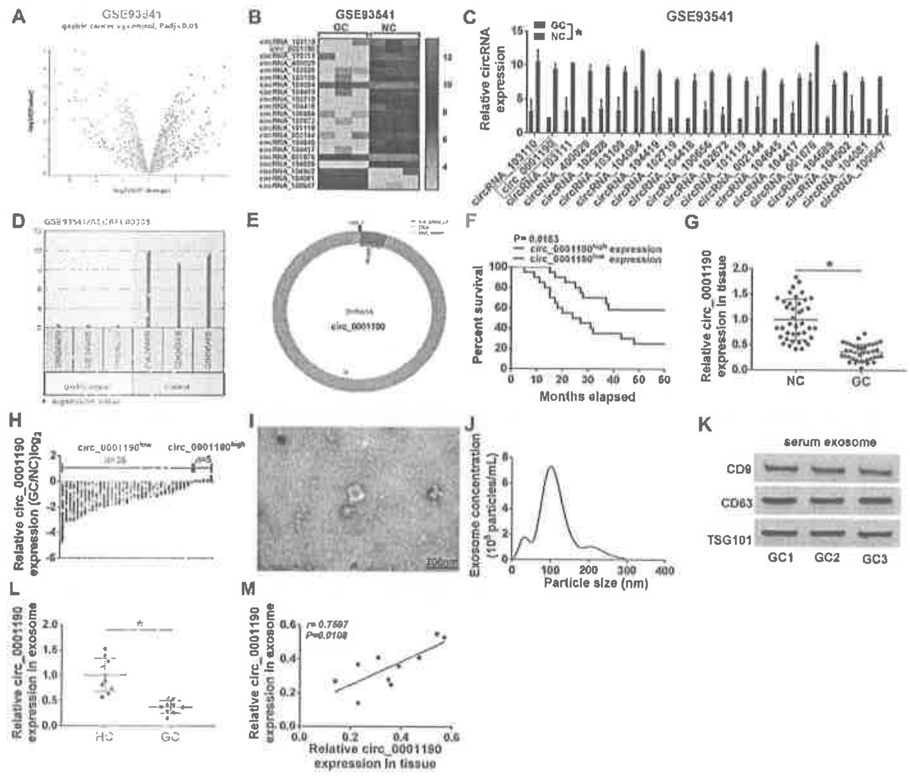

Fig. 1 Expression and validation of circ_0001190 in GC tissues and serum exosomes. **A** Volcano plot displayed circRNAs that altered prominently between GC tissues and matched normal tissues. **B** Cluster heat map presented the dissimilarly expressed circRNAs in paired human GC tissues and normal tissues. **C** The expression of circRNAs was assessed by qRT-PCR in paired human GC tissues and normal tissues. **D** The expression of circ_0001190 was examined by qRT-PCR. **E** The structure of circ_0001190. **F** The survival rate of GC patient. **G** and **H** The relative levels of circ_0001190 in GC tissues were detected by qRT-PCR. **I** Scanning of exosomes isolated from human plasma using electron microscopy. **J** NTA of plasma exosomes. **K** WB analysis of exosomal markers. **L** The relative levels of circ_0001190 in GC serum exosomes were examined by qRT-PCR. **M** Pearson's correlation analysis established that circ_0001190 in tissue was positive linked with circ_0001190 in exosome ($R = 0.7597$) in GC tissues. $^*P < 0.05$

Results

Expression and Validation of circ_0001190 in GC Tissues and Serum Exosomes

Firstly, the GSE93541 database was used for the study. The volcano map showed that circRNAs that changed pointedly between GC and corresponding normal tissues (Fig. 1A). The cluster heat map shown in Fig. 1B indicated that circ_0001190 abundance was dramatically lesser in GC tissues. All the circRNA in this cluster heat map were differentially expressed (|log2FC|> 5 and $P<0.05$) between GC tissues and normal tissues. From the eligible circRNA (|log2FC|> 5 and $P<0.05$) in the GSE93541 database, we selected circ_0001190, which has a large difference in expression, to conduct a detailed study (Fig. 1C). Besides, in GSE93541 database, the expression of circ_0001190 was downregulated in GC tissues (Fig. 1D). Figure 1E showed that the circ_0001190 was a ring structure. Besides, among 40 GC patients, the group with low circ_0001190 expression had a relatively low survival rate compared with the group with high circ_0001190 (Fig. 1F). The results revealed that circ_0001190 was associated with the prognosis of GC. The circ_0001190 level was lower in GC tumor tissues ($n=40$) compared with that in para-cancerous tissues ($n=40$) (Fig. 1G). Then, the abundance of circ_0001190 in 40 paired GC tissues and para-cancerous tissues was detected. The circ_0001190 was downregulated in 35 GC tissues (Fig. 1H). Whereafter, we separated plasma exosomes from GC sufferers and normal subjects, and these exosomes were first analyzed by electron microscopy (Fig. 1I). The exosomes were about 100 nm in diameter, which was a typical size for exosomes (Fig. 1J). The exosomal markers CD9, CD63, and TSG101 were obviously measured in exosomes from all groups (Fig. 1K). The circ_0001190 level in exosome was abnormally lower in GC patient's plasma ($n=10$) compared with that in healthy person's plasma ($n=10$) (Fig. 1L). Pearson's correlation analysis unfolded that the circ_0001190 abundance in exosome was positive correlated with the circ_0001190 level in tissue (Fig. 1M). These results suggested that circ_0001190 was a downregulated circRNA derived from GC tissues and could be effectively delivered by exosomes into the circulation. Furthermore, a low abundance of circ_0001190 was linked with poor prognosis of GC, making it a possible marker of GC.

Expression and Validation of circ_0001190 in GC Cells and Cell Exosomes

We reconnoitered whether the abundance of circ_0001190 was unusual in GC cells and cell exosomes. The circ_0001190 level was evidently lower in GC cell lines (HGC27, AGS, MKN45, MKN47 and N87) compared with that in GES-1 cells (Fig. 2A). Among them, the level of circ_0001190 was lower in HGC27 and AGS cells, so they were used for subsequent experiments. Whereafter, we isolated GES-1, HGC27 and AGS cell lines exosomes and these exosomes were first examined by electron microscopy (Fig. 2B). The exosomes were about 100 nm in diameter, which was a typical size for exosomes (Fig. 2C).

12

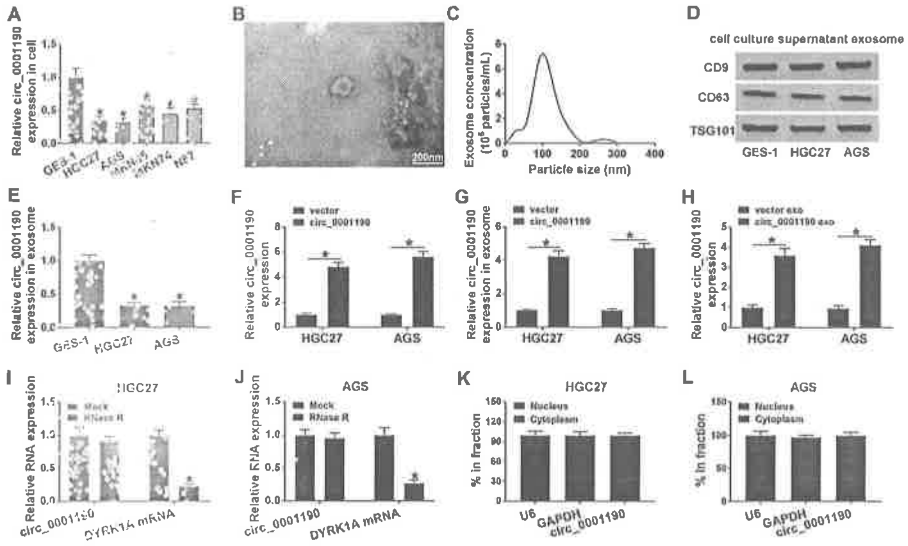

Fig. 2 Expression and validation of circ_0001190 in GC cells and cell exosomes. A The abundance of circ_0001190 in GC cells was quantified by qRT-PCR. B Scanning of exosomes isolated from GC cells using electron microscopy. C NTA of GC cells exosomes. D WB analysis of exosomal markers. E The relative content of circ_0001190 in GC cells exosome was distinguished by qRT-PCR. F and G The overexpression competence of circ_0001190 was measured by qRT-PCR. H The relative level of circ_0001190 was identified by qRT-PCR. I and J The relative levels of circ_0001190 and DYRK1A mRNA were assessed by qRT-PCR. K and L The relative level of circ_0001190 was exposed by qRT-PCR. *$P < 0.05$

The exosomal markers CD9, CD63, and TSG101 were examined in exosomes from all groups (Fig. 2D). The qRT-PCR assay assessed that the circ_0001190 expression in exosome was dramatically lower in HGC27 and AGS cells versus that in GES-1 cells (Fig. 2E). In addition, circ_0001190 expression was memorably increased transfected with circ_0001190 compared to the vector group in HGC27 and AGS cells or cell exosomes (Fig. 2F and G). Meanwhile, the above overexpressed exosomes incubated with GC cells could increase the expression of circ_0001190 in GC cells (Fig. 2H). Preceding studies have shown, RNase R does not abridgment circular RNAs but only linear RNAs. As displayed in Fig. 2I and J, after the supplement of RNase R, the abundance of DYRK1A mRNA was significantly abridged, while the content of circ_0001190 was not changed. The consequence uncovered the cyclic structure of circ_0001190. Additionally, the content of circ_0001190 in cytoplasm was higher than that in nucleus (Fig. 2K and L). These outcomes exposed that circ_0001190 was down-regulation in GC cells, which could be delivered by exosomes into the circulation to take influence in GC. In addition, circ_0001190 structure was confirmed circular RNA.

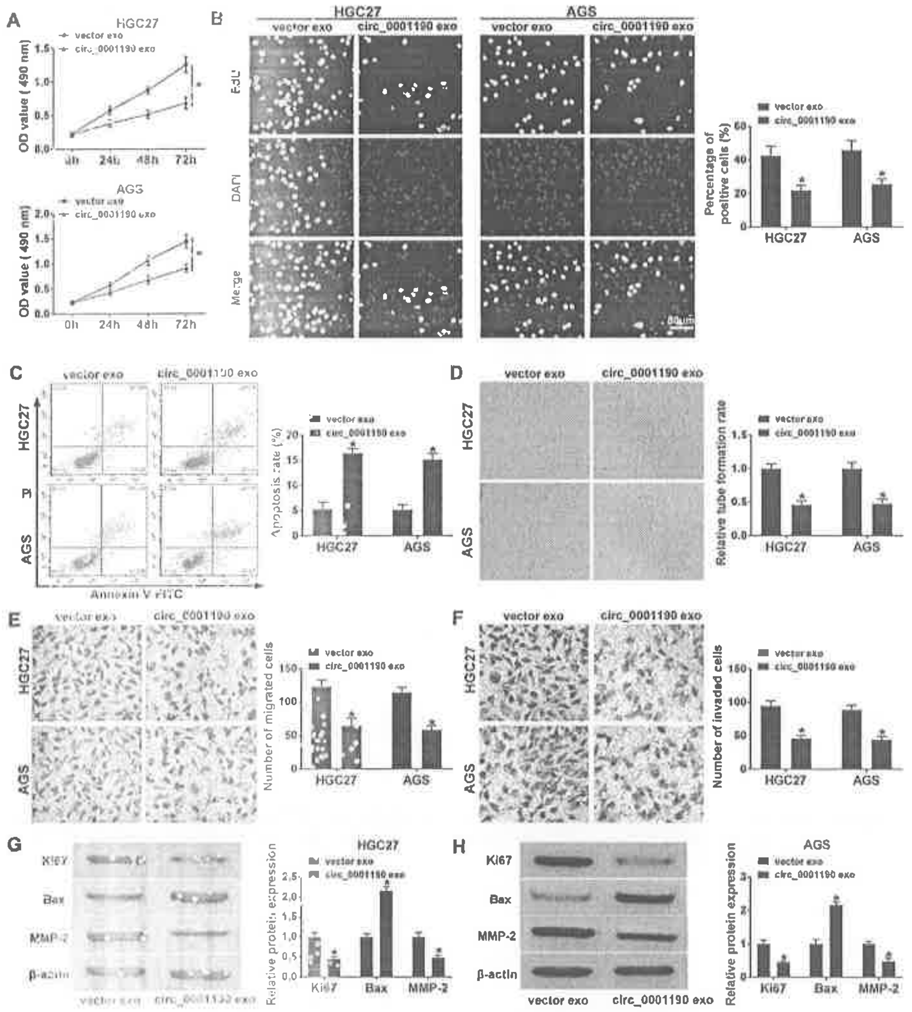

Fig. 3 Circ_0001190 subdued GC progression. **A** The CCK8 assay unfolded the cell vitality. **B** The EdU assay showed the cell proliferation. **C** The cell apoptosis was spotted by flow cytometry assay. **D** The tube formation assay detected the cell angiogenesis. **E** and **F** The transwell assay measured the cell migration and invasion. **G** and **H** The contents of Ki67, Bax, and MMP-2 were quantified by western blot. *$P < 0.05$

Exosomal of circ_0001190 Overexpression Inhibited Cell Vitality, Cell Proliferation, Angiogenesis, Cell Migration and Invasion, Whereas Promoted Cell Apoptosis in GC Cells

Hence, to discover the character of circ_0001190 in GC, the functional assay was implemented. Figures 3A showed that circ_0001190 exo could remarkably decreased the cell vitality. In addition, the consequences of EdU assay discovered the circ_0001190 exo inhibited cell proliferation (Fig. 3B). In addition, the results

14

of flow cytometry assay uncovered the circ_0001190 exo promoted cell apoptosis (Fig. 3C). Moreover, the tube formation assay unfold that circ_0001190 exo suppressed the cell ability of angiogenesis (Fig. 3D). Meanwhile, transwell assay showed that circ_0001190 exo could restrain the cell migration and invasion in GC cells (Fig. 3E and F). Ki67, Bax and MMP-2 are associated with cell proliferation, apoptosis and cell migration, respectively. Here, we verified that circ_0001190 exo abridged the levels of Ki67 and MMP-2, but improved the content of Bax in GC cells (Fig. 3G and H). Our results indicated that exosomal of circ_0001190 overexpression inhibited cell vitality, cell proliferation, angiogenesis, cell migration and invasion, whereas endorsed cell apoptosis in GC cells.

MiR-586 Acted as the Target of circ_0001190 in GC Cells

Circinteractome and circbank predicted that the target miRNAs of circ_0001190 (Fig. 4A). The two databases predicted overlapping results for six miRNAs, comprising miR-576-5p, miR-586, miR-512-5p, miR-1827, miR-568, and miR-665. Among them, the expression of miR-586 had the most significant upregulated in GC tumor tissues ($n=3$) versus that in normal tissues ($n=3$) (Fig. 4B). Therefore,

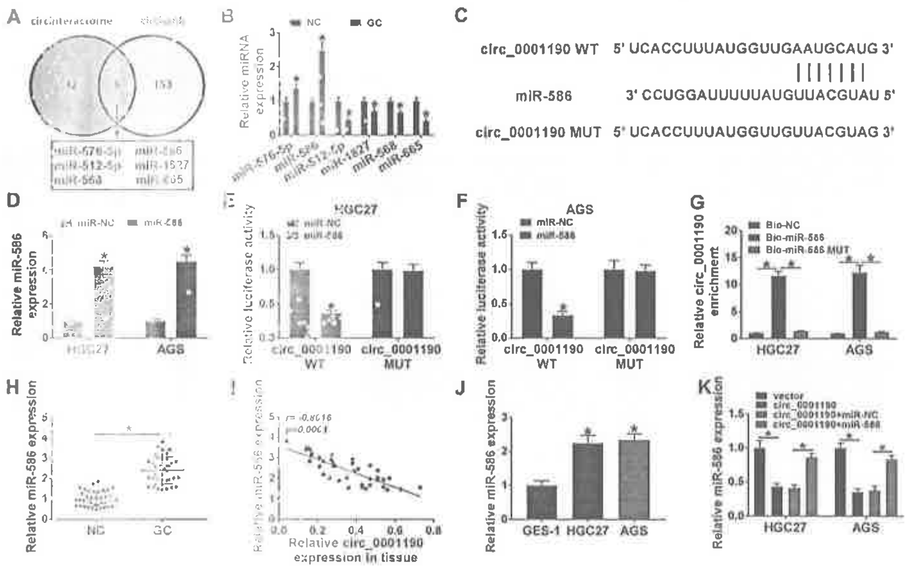

Fig. 4 Circ_0001190 sponged miR-586. **A** The targeted miRNAs of circ_0001190 were estimated by circinteractome and circbank. **B** The expressions of miRNAs were perceived by qRT-PCR. **C** The binding sites of miR-586 and circ_0001190. **D** The expression of miR-586 in GC cells was assessed by qRT-PCR. **E** and **F** Dual-luciferase reporter assay was utilized to confirm the association between circ_0001190 and miR-586. **G** RNA pull-down assay was exposed to substantiate the connection between circ_0001190 and miR-586. **H** The relative levels of miR-586 in GC tissues were measured by qRT-PCR. **I** Pearson's correlation analysis uncovered that circ_0001190 in tissue was negatively linked with miR-586 ($R = -0.8016$) in GC tissues. **J** and **K** The expression of miR-586 in GC cells was measured. $*P < 0.05$

miR-586 was used for follow-up research. Figure 4C showed the binding sites of miR-586 and circ_0001190. Besides, the miR-586 expression was markedly increased by miR-586 mimic in GC cells (Fig. 4D). The luciferase activity was diminished in circ_0001190 WT and miR-586 mimic co-transfected in GC cells compared to circ_0001190 WT and miR-NC co-transfected, but there was no difference in circ_0001190 MUT and miR-586 mimic co-transfection groups (Fig. 4E and F). The RNA pull-down assay confirmed the straight mutuality between miR-586 and circ_0001190 in GC cells (Fig. 4G). In addition, the miR-586 was upregulated in GC tumor tissues ($n=40$) versus that in normal tissues ($n=40$) (Fig. 4H). Pearson's correlation analysis unfolded that the circ_0001190 content in tissue was negative correlated with the miR-586 expression in tissue (Fig. 4I). The miR-586 abundance was higher in GC cell lines (HGC27 and AGS) compared with that in GES-1 cells (Fig. 4J). Moreover, our data also suggested that the miR-586 expression was markedly declined by circ_0001190 overexpression, but augmented by miR-586 mimic (Fig. 4K).

MiR-586 Mimic Reversed circ_0001190 Exo Induced Inhibition in GC Cells

The miR-586 expression was markedly decreased by circ_0001190 exo, but increased by miR-586 mimic (Fig. 5A). Functionally, circ_0001190 exo inhibited the cell proliferation, but miR-586 mimic could diminish the impact in GC cells

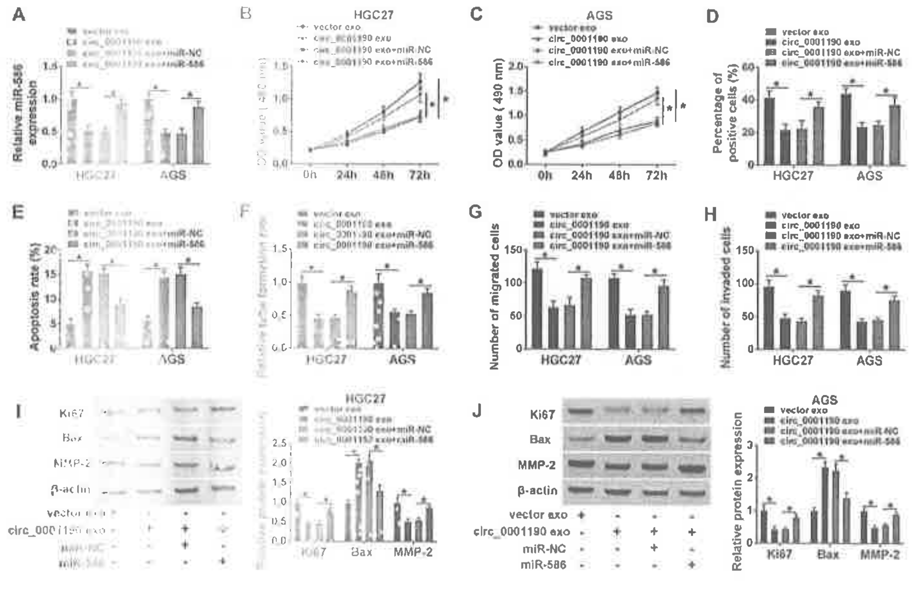

Fig. 5 Circ_0001190 subdued the advancement of GC by miR-586. **A** The miR-586 level was distinguished by qRT-PCR. **B** and **C** The cell vitality, **D** the cell proliferation, **E** the cell apoptosis, **F** the cell angiogenesis, **G** and **H** the cell migration and invasion, **I** and **J** the protein levels of Ki67, Bax, and MMP-2 were inspected by CCK8 assay, EdU assay, flow cytometry assay, tube formation assay, transwell assay, and western blot. $*P < 0.05$

(Fig. 5B–D). Besides, circ_0001190 exo promoted cell apoptosis, but miR-586 mimic could impair the impact in GC cells (Fig. 5E). Moreover, the circ_0001190 exo suppressed the cell ability of angiogenesis, whereas miR-586 mimic could lessen the impact in GC cells (Fig. 5F). Meanwhile, the circ_0001190 exo could restrain the cell migration and invasion, but miR-586 mimic could weaken the impact in GC cells (Fig. 5G and H). Besides, miR-586 mimic could inhibit the effect of circ_0001190 exo on the level of Ki67, Bax and MMP-2 in GC cells (Fig. 5I and J). Our consequences designated that circ_0001190 exo inhibited the growth of GC cells, whereas miR-586 mimic could lessen the impact.

MiR-586 Targeted SOSTDC1 in GC Cells

In GSE158662 database, only one eligible ($\log_2FC < -4$, $P < 0.05$) mRNA overlapped with TargetScan predicted miR-586 targeted mRNA, which was SOSTDC1 (Fig. 6A). Figure 6B shows the binding sites of miR-586 in SOSTDC1 3'UTR. The luciferase activity of SOSTDC1 3'UTR WT group was effectively reduced after miR-586 mimic transfection. Though, the luciferase activity of SOSTDC1 3'UTR MUT group was not altered by miR-586 (Fig. 6C and D). Our data also suggested that SOSTDC1 was downregulated in GC tumor tissues ($n=40$) compared with that in normal tissues ($n=40$) (Fig. 6E). In STAD based (http://ualcan.path.uab.edu/cgibin/TCGAExResultNew2.pl?genenam=

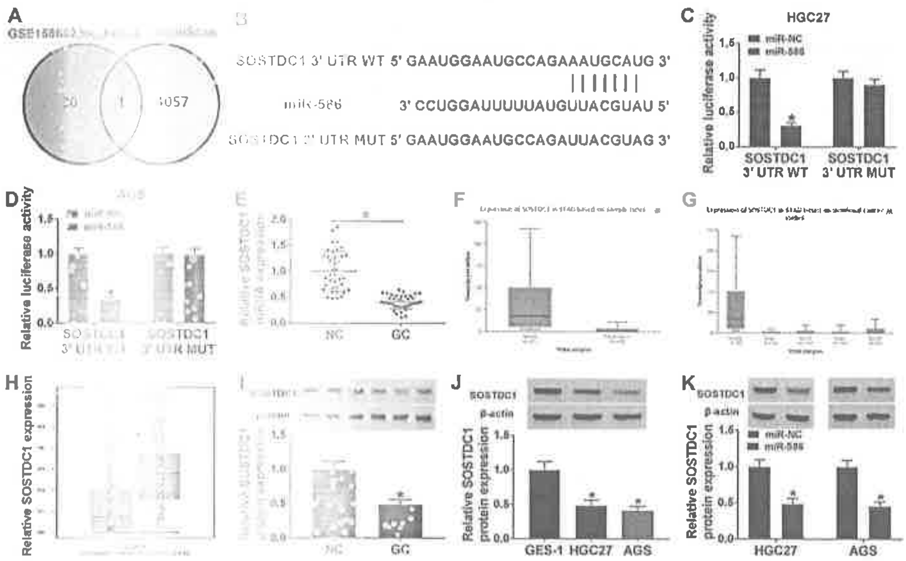

Fig. 6 MiR-586 targeted SOSTDC1 in GC cells. **A** The targeted gene of miR-586 was forecast by TargetScan. **B** The combinative sites between miR-586 and SOSTDC1. **C** and **D** Dual-luciferase reporter assay was adopted to check the link between miR-586 and SOSTDC1. **E** The SOSTDC1 content was detected by qRT-PCR. **F–H** The abundance of SOSTDC1. **I–K** The level of SOSTDC1 was detected by western blot. $^*P<0.05$

16

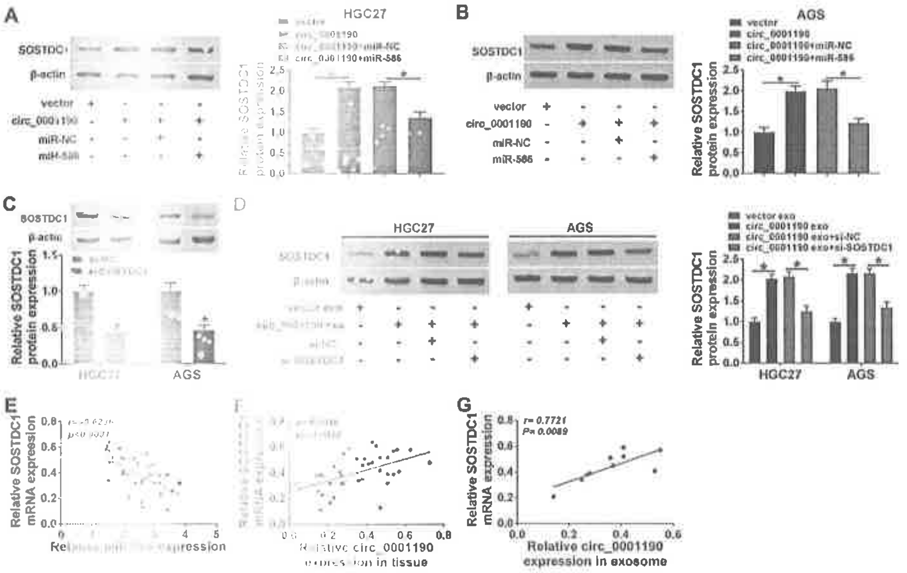

Fig. 7 Abundance of SOSTDC1 was adjusted by circ_0001190 and miR-586. **A–D** The expression of SOSTDC1 was distinguished by western blot. **E** Pearson's correlation analysis established that the level of SOSTDC1 was negatively linked with miR-586 (R=-0.6236) in GC tissues. **F** Pearson's correlation analysis exposed that circ_0001190 in tissue was positively associated with SOSTDC1 (R=0.5016) in GC tissues. **G** Pearson's correlation analysis revealed that circ_0001190 in exosome was positive linked with SOSTDC1 (R=0.7721) in GC tissues. *$P<0.05$

SOSTDC1&type=STAD), we found that the SOSTDC1 was downregulated in GC tumor tissues ($n=415$) compared with that in normal tissues ($n=34$) (Fig. 6F and G). In GEPIA based, we found that the SOSTDC1 was downregulated in GC tumor tissues ($n=408$) compared with that in normal tissues ($n=211$) (Fig. 6H). Figures 6I and J show that the protein level of SOSTDC1 was downregulated in GC tumor tissues ($n=3$) and cells (HGC27 and AGS) compared with that in normal tissues ($n=3$) and GES-1 cells. In addition, the SOSTDC1 content was diminished by transfected miR-586 mimic in GC cells (Fig. 6K). Furthermore, the level of SOSTDC1 was increased by transfected circ_0001190, but decreased by miR-586 mimic in GC cells (Fig. 7A and B). The SOSTDC1 protein level was markedly decreased by si-SOSTDC1 in GC cells (Fig. 7C). Meanwhile, the SOSTDC1 protein level was markedly increased by circ_0001190 exo, whereas decreased by si-SOSTDC1 in GC cells (Fig. 7D). Pearson's correlation analysis unfolded that the SOSTDC1 mRNA level in tissue was negative correlated with the miR-586 content in tissue (Fig. 7E). As the same way, the SOSTDC1 mRNA abundance in tissue was positive correlated with the circ_0001190 level in tissue (Fig. 7F). Besides, the SOSTDC1 mRNA expression in serum was positive correlated with the circ_0001190 expression in exosome (Fig. 7G). Collectively, these discoveries suggested that circ_0001190 promoted the expression of SOSTDC1 via miR-586.

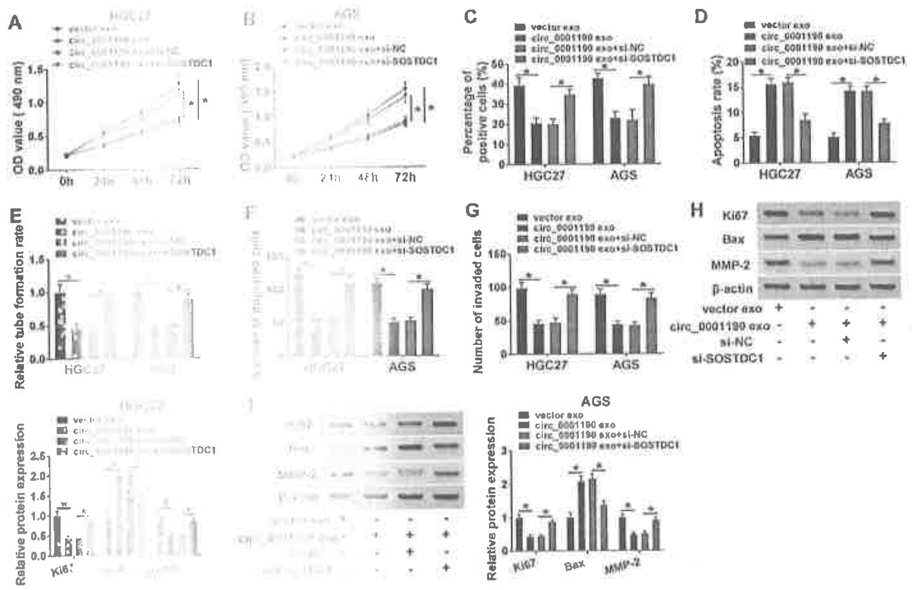

Fig. 8 Circ_0001190 adjusted the advancement of GC by regulating SOSTDC1. **A** and **B** The cell vitality, **C** the cell proliferation, **D** the cell apoptosis, **E** the cell angiogenesis, **F** and **G** the cell migration and invasion, **H** and **I** the protein contents of Ki67, Bax, and MMP-2 were examined by CCK8 assay, EdU assay, flow cytometry assay, tube formation assay, transwell assay, and western blot. *$P < 0.05$

Silencing SOSTDC1 Reversed circ_0001190 Exo Induced Inhibition in GC Cells

Functionally, circ_0001190 exo inhibited cell proliferation, but SOSTDC1 deficiency could lessen the impact (Fig. 8A–C). Besides, circ_0001190 exo promoted cell apoptosis, but silencing SOSTDC1 could lessen the impact in GC cells (Fig. 8D). Moreover, the circ_0001190 exo reduced the cell ability of angiogenesis, whereas si-SOSTDC1 could lessen the impact in GC cells (Fig. 8E). Meanwhile, the circ_0001190 exo could restrain the cell migration and invasion, but SOSTDC1 deficiency could weaken the impact in GC cells (Fig. 8F and G). Besides, si-SOSTDC1 could inhibit the effect of circ_0001190 exo on the level of Ki67, Bax and MMP-2 in GC cells (Fig. 8H and I). Our results indicated that silencing SOSTDC1 could reverse circ_0001190 exo induced inhibition in GC cells growth.

Circ_0001190 Exo Restricted Tumor Growth In vivo

As shown in Fig. 9A–C, circ_0001190 exo treatment repressed tumor volume and weight. Then, the tumor tissues were examined. The circ_0001190 exo increased the level of circ_0001190, SOSTDC1, and Bax, but repressed the expression of miR-586, Ki67, and MMP-2 (Fig. 9D and E). The outcomes from IHC exposed that the abundance of Ki67 was lower, but SOSTDC1 was higher in the circ_0001190 exo

18

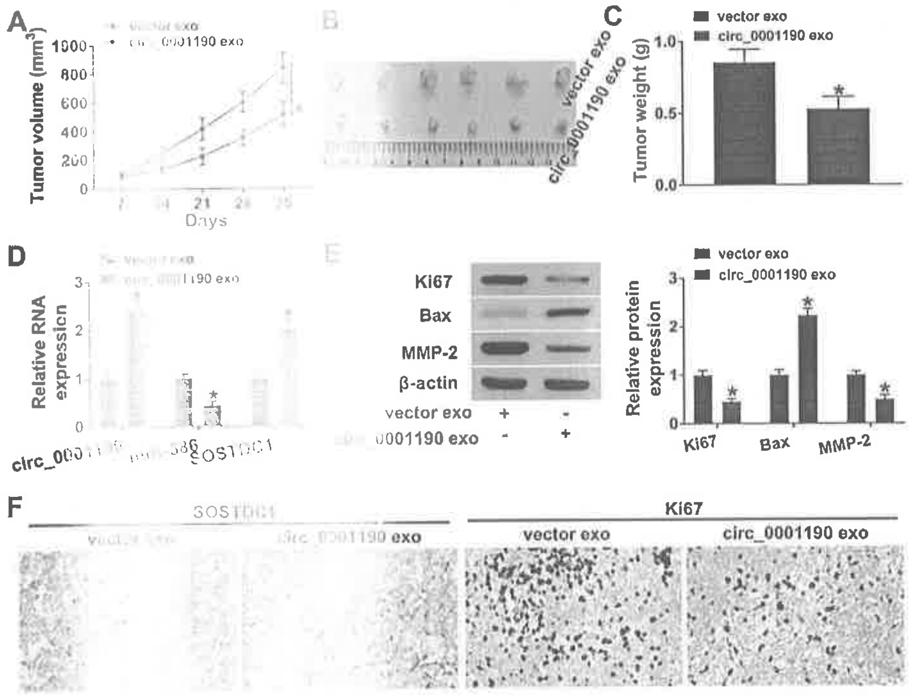

Fig. 9 Circ_0001190 restricted tumor growth. A–C The tumor volume and weight was assessed. D The abundances of circ_0001190, miR-586, and SOSTDC1 were discovered by qRT-PCR. E The contents of Ki67, Bax, and MMP-2 in these excised tumor tissues were detected by western blot. F IHC was applied to inspect the Ki67 and SOSTDC1 levels. *$P < 0.05$

group compared with that in vector exo group (Fig. 9F). These consequences signposted that circ_0001190 exo repressed xenograft tumor growth.

Discussion

In current clinical practice, advanced GC was mainly treated by surgery (He et al. 2015). With the development of GC research, the emergence of many new targeted drugs has provided new ideas for the treatment (Shen et al. 2015; Zhang et al. 2015). Many molecular targeted agents have demonstrated significant antitumor activity in lots of molecular pathways, such as cell growth, cell cycle, angiogenesis, and invasion, providing molecular targets for cancer therapy (Huang et al. 2014; Lin et al. 2017). However, the functions of circ_0001190 in GC were still uncertain. Hence, our paper inspected the character of circ_0001190.

In our paper, we exposed that the circ_0001190 was downregulated in the GC, which is parallel to Liu et al. discoveries (Liu et al. 2020). Besides, circRanGAP1 regulated VEGFA abundance by binding miR-877-3p to elevate GC cell metastasis (Lu et al. 2020). Moreover, hsa_circ_0000745 was reduced in GC

19

and linked with GC cells differentiation (Huang et al. 2017). In addition, circ-DONSON facilitated GC growth, invasion, and apoptosis (Ding et al. 2019). Hsa_circ_[illegible] curbed GC development by interfering miR-197-3p (Sun et al. 2021). Herein, our consequences signposted that exosomal circ_0001190 overexpression inhibited cell vitality, cell proliferation, angiogenesis, cell migration and invasion, whereas promoted cell apoptosis in GC cells. Our results were similar to those of our predecessors. The circRNAs could competitively sponge for miRNAs, like circ_0004872 could target miR-224 in GC (Ma et al. 2020). In this study, exosomal circ_0001190 overexpression inhibited the progression of GC by sponging miR-586, which was parallel to former discoveries.

According to preceding information, miR-586 was relevant to the progress of glioma ([illegible] et al. 2020; Yang et al. 2015). In addition, miR-586 served as an oncogene via accelerating breast cancer (BC) growth and metastasis via ZEB1 (Zhang et al. 2021). Moreover, miR-586 might link with the risk of cervical cancer (Yu et al. 2020). Beyond that, miR-586 took part in adjusting the nephrotic syndrome development (Teng et al. 2015). In this paper, we discovered that miR-586 promoted the progress of GC by targeting SOSTDC1. This regulation mode was consistent with previous studies (Zhang et al. 2021). At present, many researches have proved that SOSTDC1 was associated with the development of BC, GC and kidney cancer (Rawat and Gopisetty 2014; Gopal et al. 2013; Blish et al. 2009). Also, SOSTDC1 could contribute to cell invasion in colorectal cancer (Bartolome et al. 2020). In addition, BMP could antagonist SOSTDC1 to block GC development (Cui et al. 2019). Besides, SOSTDC1 served as a tumor-suppressive factor in GC and downregulation of it promoted tumor growth and boosted the formation of lung metastasis (Cui et al. 2019). In this paper, we got the same result as Cui et al. (Cui et al. 2019). In this research, the level of SOSTDC1 was downregulation in GC. Meanwhile, we witnessed that miR-586 reversed the increase effect of circ_0001190 on SOSTDC1 expression in GC cells. These outcomes additional sustained the control circuit of the circ_0001190/miR-586/SOSTDC1 in GC cells.

In brief, the paper demonstrated that circ_0001190 and SOSTDC1 were downregulated and miR-586 was upregulated in GC. Furthermore, our study manifested that exosomal circ_0001190 overexpression inhibited cell vitality, cell proliferation, angiogenesis, cell migration and invasion, whereas promoted cell apoptosis in GC cells via miR-586/SOSTDC1 axis. There are still some limitations to the study, such as these data need further studied in clinical practice. Overall, this study provides clues to the regulatory mechanisms of GC and opens up new potential therapeutic avenues for future clinical targeted therapy.

Acknowledgements Not applicable.

Funding None.

Declarations

Conflict of interest The authors declare that they have no conflicts of interest.

Refere[illegible]

Ahn Y et al [illegible] function in modulation of Wnt/beta-catenin signaling during tooth [illegible]2824–2836

Allemani [illegible] of trends in cancer survival 2000–14 (CONCORD-3): analysis of [illegible] patients diagnosed with one of 18 cancers from 322 population-[illegible] Lancet 391:1023–1075

Ambros V [illegible] microRNAs. Nature 431:350–355

Bartolome [illegible] promotes invasion and liver metastasis in colorectal cancer via inter[illegible] Oncogene 39:6085–6098

Blish KR [illegible] morphogenetic protein antagonist is down-regulated in renal cancer. Mol [illegible]

Bray F et al [illegible] 2018: GLOBOCAN estimates of incidence and mortality worl[illegible]ries. CA Cancer J Clin 68:394–424

Chen G et [illegible] metastasis in non-small cell lung cancer and may serve as a clini[illegible] 42:3424–3436

Cui Y et [illegible]OSTDC1, restrains gastric cancer progression via inactivation of c-[illegible]:2331–2348

Ding L et [illegible]-DONSON facilitates gastric cancer growth and invasion via NUR[illegible] of transcription factor SOX4. Mol Cancer 18:45

Garzon R, [illegible] targeting microRNAs in cancer: rationale, strategies and challeng[illegible]

Gopal G, [illegible] KR, Rajkumar T (2013) SOSTDC1 down-regulation of expr[illegible] and is a potential prognostic marker in gastric cancer. Cancer Gen[illegible]

He W et a[illegible] gastric cancer: a review of systematic reviews. Int J Clin Exp Med [illegible]

Hou W, [illegible] promotes the progression of ovarian cancer by activating the expr[illegible] miR-184. Pathol Res Pract 217:153275

Huang J, [illegible] generating gene family member 4 promotes growth and migration [illegible] kinase B pathway. Int J Clin Exp Med 7:3037–3044

Huang M, [illegible] ZQ (2017) Circular RNA hsa_circ_0000745 may serve as a diag[illegible] World J Gastroenterol 23:6330–6338

Lee HS e[illegible] Gastrointestinal Cancer. J Pathol Transl Med 51:103–121

Li T et al [illegible] profiling of patients with gastric cancer and their droplet digital RT-[illegible] 96:85–96

Liang M [illegible] hsa_circ_006100 in gastric cancer promote cell growth and meta[illegible] signalling. Cell Prolif 52:e12661

Lin Y et [illegible] signaling promotes cell proliferation through a PLC-dependent pathway [illegible] efficacy in gastric cancer. Oncotarget 8:11990–12002

Liu J, Li [illegible] ation of downregulated circRNAs from tissue and plasma of patie[illegible] uction of a circRNA-miRNA-mRNA network. J Cell Biochem [illegible]

Lu J et al [illegible] 1 regulates VEGFA expression by targeting miR-877-3p to facil[illegible] metastasis. Cancer Lett 471:38–48

Luo Y et [illegible] markers related to glioma prognosis. Eur Rev Med Pharmacol Sci [illegible]

Ma C et a[illegible]0004872 inhibits gastric cancer progression via the miR-224/Sma[illegible] circuit. Mol Cancer 19:157

Narhi K [illegible] size and number of skin appendage placodes. Dev Biol 364:[illegible]

Qiu D e[illegible] ubiquitination and promotes gastric cancer metastasis. Biochim[illegible]:1552–1561

Rawat A, [illegible] E4BP4 is a repressor of epigenetically regulated SOSTDC1 exp[illegible] Oncol (dordr) 37:409–419

Shen Z e[illegible] miR-300 in gastric cancer and its effects on cells malignancy. Int J Cli[illegible]

Shigetani Y et al (200[illegible]) [illegible] promotes coalescence of cells of neural crest and placode origins in the trigeminal region [illegible] head development. Dev Biol 319:346–358

Song Z, Wu Y, Yang [illegible] D, Fan [illegible] (2017) Progress in the treatment of advanced gastric cancer. Tumour Biol 39:1[illegible]

Sun Z et al (2015) [illegible] factors associated with splenic hilar lymph node metastasis in patients with advanced gastric [illegible] in northwest China. Int J Clin Exp Med 8:21358–21364

Sun D, Wang G, Xiao [illegible] (2021) Hsa_circ_001988 attenuates GC progression in vitro and in vivo via sponging miR-[illegible] J Cell Physiol 236:612–624

Teng J et al (2015) Differential microRNA expression in the serum of patients with nephrotic syndrome and clinical correl[illegible] analysis. Int J Clin Exp Pathol 8:7282–7286

Wang Q, Yu [illegible] (2018) [illegible] suppresses gastric cancer cell invasion and proliferation by inhibiting COL1A1. Biochem [illegible]

Wang GJ, [illegible] (2020a) Circ_0000190 suppresses gastric cancer progression potentially via inhibiting [illegible] pathway. Cancer Cell Int 20:351

Wang Z, [illegible] Zhou [illegible] (2020) CircRNA RNF111 regulates the growth, migration and invasion of gastric cancer [illegible] miR27b3p. Int J Mol Med 46:1873–1885

Xie M et al (2020) [illegible] promotes gastric cancer progression via regulating the miR-582-3p/[illegible] axis and suppressing HSP90 degradation. Mol Cancer 19:112

Yang L et al (2015) [illegible] microRNA-586 Inhibits Proliferation, Invasion and Metastasis and Promotes [illegible] in Human Osteosarcoma U2-OS Cell Line. Cytogenet Genome Res 146:[illegible]

Yu A et al (20[illegible]) [illegible] Single Nucleotide Polymorphisms of an miRNA Binding Site in the 3′ [illegible] Cervical Cancer Among the Han Chinese. Genet Test Mol Biomark[illegible]

Zhang ZZ et al (2015) [illegible] plasma MicroRNAs to identifying early diagnostic molecule for gastric [illegible] J Clin [illegible] 3706

Zhang D [illegible] (2021) [illegible] 89-[illegible]586-ZEB1 feedback loop regulates breast cancer progression through [illegible] signaling pathway. Mol Ther Nucleic Acids 25:455–467

Zheng P et al (2017) Exosomal transfer of tumor-associated macrophage-derived miR-21 confers cisplatin resistance in gastric cancer [illegible] J Exp Clin Cancer Res 36:53

Zhou Q et al (2017) [illegible] inhibits follicular thyroid cancer cell proliferation, migration, and EMT via [illegible] and MAPK/Erk signaling pathways. Mol Cell Biochem 435:87–95

22

报告编号：2022a06121

收录检索报告

委托内容：刘超发表的论文

委托机构：保定市第二医院

委托日期：2022 年 6 月 10 日

检索机构（盖章）：河北省科学技术情报研究院

（国家一级科技查新咨询单位）

检索完成日期：2022 年 6 月 10 日

23

一、检索要求：

1、被检作者：刘超

2、委托机构：保定市第二医院

二、检索范围：

Science Citation Index Expanded （SCI-EXPANDED）…………2009-present

三、检索结果：

提供的待检论文中有 1 篇被 SCI 收录：

Accession Number：YW2CR

Exosomal circ_0001190 Regulates the Progression of Gastric Cancer via miR-586/SOSTDC1 Axis

By: 刘超（Liu, Chao；第一作者）

BIOCHEMICAL GENETICS Published: 2022

影响因子：1.890（2020）

引用 1 次，他引 1 次

检索人: 王雷鸣

河北省科学技术情报研究院

2022 年 6 月 10 日

河北省科学技术情报研究院 科技查新专用章

SCI 收录：

Exosomal circ_0001190 Regulates the Progression of Gastric Cancer via miR-586/SOSTDC1 Axis

By: Liu, Chao; Yang, Jing; Zhu, Fengchi; Zhao, Zhiying; Gao, Lixue

BIOCHEMICAL GENETICS
DOI: 10.1007/s10528-021-10180-6
Published: 2022

Abstract: Gastric cancer (GC) is the fifth most common cancer, which has a significant impact on human health. Recent researches have shown that circular RNAs (circRNAs) could affect the progress of GC, but the mechanism still indistinct. In this work, we explored the roles of circ_0001190 in GC. The levels of circ_0001190, microRNA-586 (miR-586) and sclerostin domain containing 1 (SOSTDC1) were detected by quantitative RT-PCR and western blot in GC. The cell functions were scrutinized by cell counting kit-8 assay, 5-Ethynyl-29-deoxyuridine assay, flow cytometry assay, tube formation assay, transwell assay, and western blot. Furthermore, the relationship between miR-586 and circ_0001190 or SOSTDC1 was identified by dual-luciferase reporter assay. Finally, the xenograft model test was implemented to demonstrate the effect of exosomal circ_0001190 in vivo. The levels of circ_0001190 and SOSTDC1 were downregulated, and the miR-586 level was increased in GC. For functional assay, circ _0001190 overexpression inhibited cell vitality, cell proliferation, angiogenesis, cell migration and invasion, whereas stimulated cell apoptosis in GC cells. Circ _0001190 served as a miR-586 sponge to adjust the expression of SOSTDC1. Additionally, miR-586 could promote the advancement of GC by interfering SOSTDC1. Exosomal circ_0001190 overexpression inhibited the development of GC by miR-586/SOSTDC1 axis, which proposed a potential targeted therapy for GC cure.

Keywords
Author Keywords: Gastric cancer; Exosomal circ_0001190; miR-586; SOSTDC1
KeyWords Plus: CELL-PROLIFERATION; SOSTDC1; EXPRESSION; ANTAGONIST; MICRORNAS; MIGRATION; INVASION; MARKER

Author Information
Reprint Address: Gao, LX (通讯作者)，2 Hosp Baoding, Dept Surg Oncol, 338 Dongfeng West Rd, Baoding City 071051, Hebei, Peoples R China.
Addresses:
[Liu, Chao; Zhao, Zhiying] 2 Hosp Baoding, Dept Gastroenterol, Baoding City 071051, Hebei, Peoples R China;
[Yang, Jing; Zhu, Fengchi] 2 Hosp Baoding, Dept Anorectal Surg, Baoding City 071051, Hebei, Peoples R China;
[Gao, Lixue] 2 Hosp Baoding, Dept Surg Oncol, 338 Dongfeng West Rd, Baoding City 071051, Hebei, Peoples R China
E-mail Addresses: wkysglx@163.com

Publisher
SPRINGER/PLENUM PUBLISHERS,233 SPRING ST, NEW YORK, NY 10013 USA
Journal Information
Impact Factor: Journal Citation Reports
Categories / Classification
Research Areas: Science Citation Index Expanded (SCI-EXPANDED)
Web of Science Categories: Biochemistry & Molecular Biology; Genetics & Heredity
Document Information
Document Type: Article; Early Access
Language: English
Accession Number: YW2CR
ISSN: 0006-2928
eISSN: 1573-4927